Missouri University of Science and Technology
Scholars' Mine

Electrical and Computer Engineering Faculty Research & Creative Works

Electrical and Computer Engineering

01 Jan 2003

Multilevel Inverter-Based Dual-Frequency Power Supply

B. Diong

Keith Corzine
Missouri University of Science and Technology

S. Basireddy

Shuai Lu

Follow this and additional works at: https://scholarsmine.mst.edu/ele_comeng_facwork

Part of the Electrical and Computer Engineering Commons

Recommended Citation

B. Diong et al., "Multilevel Inverter-Based Dual-Frequency Power Supply," *IEEE Power Electronics Letters*, Institute of Electrical and Electronics Engineers (IEEE), Jan 2003.
The definitive version is available at https://doi.org/10.1109/LPEL.2004.825543

This Article - Journal is brought to you for free and open access by Scholars' Mine. It has been accepted for inclusion in Electrical and Computer Engineering Faculty Research & Creative Works by an authorized administrator of Scholars' Mine. This work is protected by U. S. Copyright Law. Unauthorized use including reproduction for redistribution requires the permission of the copyright holder. For more information, please contact scholarsmine@mst.edu.

Multilevel Inverter-Based Dual-Frequency Power Supply

Bill Diong, Keith Corzine, Sarala Basireddy, and Shuai Lu

***Abstract*—Most existing power supplies for induction heating equipment produce voltage at a single (adjustable) frequency. Recently, however, induction heating power supplies that produce voltage at two (adjustable) frequencies simultaneously have been introduced and commercialized. These represent a significant development particularly for heat-treating workpieces with uneven geometries, such as gears. Still, the existing approaches to dual-frequency voltage generation could be improved upon to achieve better control, higher efficiency, and reduced electromagnetic interference. This letter proposes the use of multilevel inverters for providing power at two frequencies simultaneously. It describes how the stepping angles for the desired output from such inverters can be determined. Furthermore, experimental results are presented as verification of the concept and to demonstrate the achievement of improved harmonic level control and reduced device switching frequency.**

***Index Terms*—Dual-frequency, harmonic elimination, multilevel inverter.**

I. Introduction

MANY industries require the heating of targeted workpiece sections as part of processes such as hardening, brazing, bonding (curing), etc. One environmental-friendly approach to such heating is by electromagnetic induction, known as induction heating. Most existing induction heating power supplies produce power at a single (adjustable) frequency. Recently, however, supplies that produce power at two frequencies simultaneously have been introduced [1]–[4] as well as commercially developed [5]. This is because for workpieces with uneven geometries, such as gears, different portions are heated dissimilarly at a single frequency and so, their processing needs two steps (to allow a frequency adjustment) using a single frequency power supply. The specific low and high frequencies applied depend upon several factors, such as material and geometry but are typically 10 kHz or more with the higher frequency being 3–30 times the lower frequency. Hence, it is desirable to supply dual-frequency power simultaneously to the induction coil to attain the optimal result in just one pass. However, drawbacks of the approach proposed by [1] include the restriction of dual-frequency production to just the first and third harmonics and the inability to independently adjust their levels and those of the adjacent (fifth, seventh, etc.) harmonics, although some incremental improvements have recently been made [2]–[4]. Drawbacks of [5] include the power loss and electromagnetic interference due to the passive components and high-frequency device switching, respectively, and also the two disparate control methods for the low-frequency and high-frequency subcircuits.

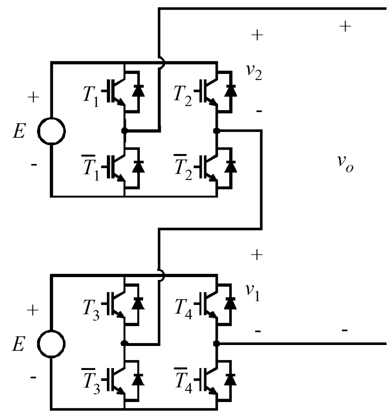

Fig. 1. Cascaded H-bridge (two-cell) multilevel inverter circuit.

This paper introduces a simultaneous dual-frequency induction heating power supply based on multilevel inverters, which may achieve improved control, higher efficiency, reduced electromagnetic interference, and greater reliability. Multilevel converters are a recent exciting development in the area of high-power systems. Several topologies exist, including the diode-clamped (neutral-point clamped), capacitor-clamped (flying capacitor), and cascaded H-bridge (see Fig. 1), etc. Presently, they are operated to produce either a staircase or pulse-width modulated approximation to a single-frequency output voltage, which could be either fixed (utility) or varying (motor drive) [6]. While [7] has introduced the idea of multilevel inverters for multifrequency induction heating, few analytical details were provided.

II. Analysis

For an output voltage staircase waveform that is quarter-wave symmetric with s positive steps of equal magnitude E, it is well-known that the waveform's Fourier series expansion is given by

$$v_o(t) = \sum_{\mathrm{odd}\,h} \{V_h \sin(h\omega t)\} \quad (1)$$

where

$$V_h = \frac{4E}{h\pi}\left[\cos(h\theta_1) + \cos(h\theta_2) + \ldots + \cos(h\theta_s)\right] \quad (2)$$

and the θ_i, $i = 1, \ldots, s$, are the angles (within the first quarter of each waveform cycle) at which the s steps occur. On the other hand, if a negative step (down) instead of a positive step (up) occurs at a particular θ_i, the coefficient of the corresponding cosine

Manuscript received December 10, 2003. Recommended by Associate Editor L. M. Tolbert.

B. Diong and S. Basireddy are with the Department of Electrical and Computer Engineering, The University of Texas at El Paso, El Paso, TX 79968 USA (e-mail: bdiong@ece.utep.edu).

K. Corzine and S. Lu are with the Department of Electrical Engineering and Computer Science, University of Wisconsin, Milwaukee, WI 53201 USA.

Digital Object Identifier 10.1109/LPEL.2004.825543

1540-7985/03$17.00 © 2003 IEEE

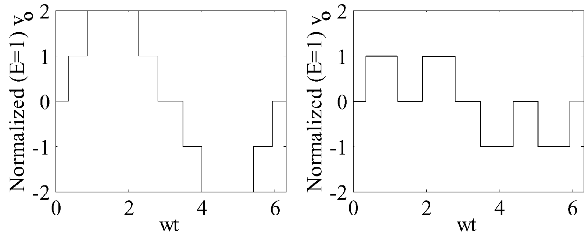

Fig. 2. Two-step waveform alternatives (PP and PN).

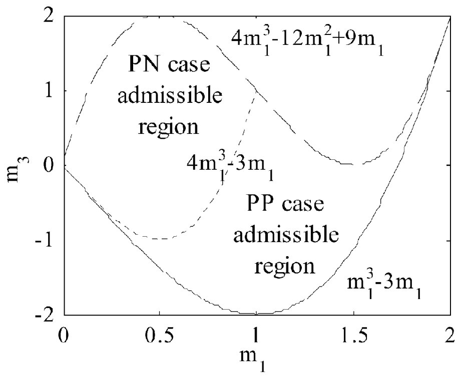

Fig. 3. Constraint curves for m_3 versus m_1 (PP and PN cases).

term in (2) is -1 instead of $+1$. Note that the even harmonics are all zero.

For the specific (introductory) problem of synthesizing a stepped waveform that has desired levels of V_1 and V_3 with two of the adjacent higher harmonics equal to zero, the stepping angles $0 \leq \theta_1 < \theta_2 < \ldots < \theta_s \leq \pi/2$ must be chosen so that

$$\frac{4E}{\pi}\left[\cos(\theta_1) + \cos(\theta_2) + \ldots + \cos(\theta_s)\right] = V_1 \quad (3a)$$

$$\frac{4E}{3\pi}\left[\cos(3\theta_1) + \cos(3\theta_2) + \ldots + \cos(3\theta_s)\right] = V_3 \quad (3b)$$

$$\cos(5\theta_1) + \cos(5\theta_2) + \ldots + \cos(5\theta_s) = 0 \quad (3c)$$

$$\cos(7\theta_1) + \cos(7\theta_2) + \ldots + \cos(7\theta_s) = 0. \quad (3d)$$

Again, for a waveform with a step down instead of a step up occurring at a particular θ_i, the coefficient of the corresponding cosine term in (3) should be -1 instead of $+1$. Using the identities (also advocated by [8])

$$\cos(3\theta) = 4\cos(\theta)^3 - 3\cos(\theta) \quad (4a)$$

$$\cos(5\theta) = 16\cos(\theta)^5 - 20\cos(\theta)^3 + 5\cos(\theta) \quad (4b)$$

$$\cos(7\theta) = 64\cos(\theta)^7 - 112\cos(\theta)^5 + 56\cos(\theta)^3 - 7\cos(\theta) \quad (4c)$$

and defining c_i as $\cos(\theta_i)$, (3) can be rewritten as

$$\sum_{i=1,\ldots,s} c_i = \frac{V_1}{\frac{4E}{\pi}} = m_1 \quad (5a)$$

$$\sum_{i=1,\ldots,s} \left\{4c_i^3 - 3c_i\right\} = \frac{V_3}{\frac{4E}{3\pi}} = m_3 \quad (5b)$$

$$\sum_{i=1,\ldots,s} \left\{16c_i^5 - 20c_i^3 + 5c_i\right\} = 0 \quad (5c)$$

$$\sum_{i=1,\ldots,s} \left\{64c_i^7 - 112c_i^5 + 56c_i^3 - 7c_i\right\} = 0. \quad (5d)$$

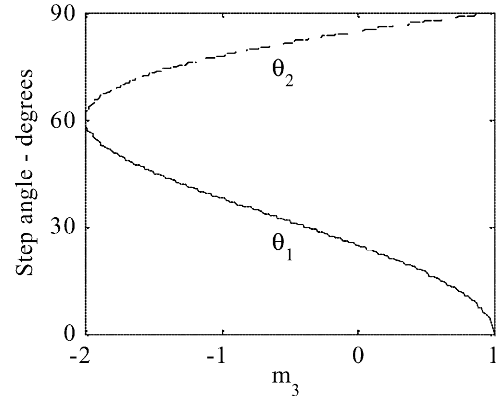

Fig. 4. Step angle solutions for $m_1 = 1$ (PP case).

Thus, the set of trigonometric equations (3) has been transformed into a set of multivariate polynomial equations (5), the solution of which, discussed in [9] for example, will yield the step angles of the inverter output voltage waveform with the desired dual-frequency content. Clearly, a necessary condition for the existence of nontrivial solutions to (5) is that the number of steps s be greater than or equal to the number of constraint equations.

In the following, the presented analysis starts with the 2-step $(s = 2)$ waveform with desired levels of first and third harmonics for simplicity. Then more practical first and fifth harmonic generation is described for both three-step waveforms with simultaneous elimination of the third and four-step waveforms with simultaneous elimination of the third and seventh.

A. Two-Step Waveform Problem

There are two alternatives to consider: the PP case and PN case representing waveforms having two successive positive steps, and a positive step followed by a negative step, respectively (see Fig. 2). Their negations, the NN case and NP case, simply result in solutions that are 180° phase-shifted, respectively, from the PP and PN solutions.

1) PP Case: The applicable equations are, from (5a) and (5b)

$$c_1 + c_2 = m_1 \quad (6a)$$

$$\left(4c_1^3 - 3c_1\right) + \left(4c_2^3 - 3c_2\right) = m_3 \quad (6b)$$

which yield

$$c_1 = \frac{\left[3m_1^2 + \sqrt{3\left(3m_1^2 - m_1^4 + m_1 m_3\right)}\right]}{6m_1} \quad (7a)$$

$$c_2 = \frac{\left[3m_1^2 - \sqrt{3\left(3m_1^2 - m_1^4 + m_1 m_3\right)}\right]}{6m_1}. \quad (7b)$$

From (6) and (7), note that for admissible c_1 and c_2 (each must be a real value between 0 and 1) m_1 is restricted to a value between 0 and 2, while m_3 is constrained so that

$$m_1^3 - 3m_1 \leq m_3 \leq 4m_1^3 - 3m_1, \quad \text{for } 0 \leq m_1 \leq 1 \quad (8a)$$

$$m_1^3 - 3m_1 \leq m_3 \leq 4m_1^3 - 12m_1^2 + 9m_1, \quad \text{for } 1 \leq m_1 \leq 2. \quad (8b)$$

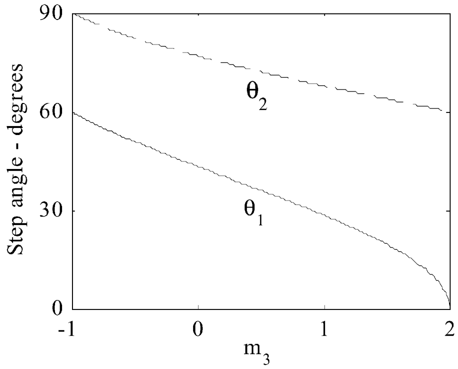

Fig. 5. Step angle solutions for $m_1 = 0.5$ (PN case).

The plot of these constraint curves in Fig. 3 for m_3 versus m_1 indicates (and confirmed analytically) that the range of possible m_3 is maximized at $m_1 = 1$. Then for $m_1 = 1$, as an example, the solutions for θ_1 and θ_2 are as shown in Fig. 4 as m_3 varies. Note that $V_3/V_1 = m_3/(3m_1)$. The solutions for θ_1 and θ_2 were also obtained at other allowable values of m_1 and m_3, but these are not shown here due to space constraints. Note also that this case requires the production of a five-level waveform and (at least) a two-cell converter. With a two-cell converter, it is possible to turn on and turn off each switch at the fundamental frequency to produce the desired waveform.

2) PN Case: For this case, the applicable equations are

$$c_1 - c_2 = m_1 \tag{9a}$$

$$\left(4c_1^3 - 3c_1\right) - \left(4c_2^3 - 3c_2\right) = m_3 \tag{9b}$$

where the second equation is obtained instead of (6b) because the second step is down instead of up. Then substituting (9a) into (9b) and solving for c_1 and c_2 yields

$$c_1 = \frac{\left[3m_1^2 + \sqrt{3\left(3m_1^2 - m_1^4 + m_1 m_3\right)}\right]}{6m_1} \tag{10a}$$

$$c_2 = \frac{\left[-3m_1^2 + \sqrt{3\left(3m_1^2 - m_1^4 + m_1 m_3\right)}\right]}{6m_1}. \tag{10b}$$

From (9) and (10), note that for admissible c_1 and c_2 (each must be a real value between 0 and 1) m_1 is restricted to a value between 0 and 1, while m_3 is constrained so that

$$4m_1^3 - 3m_1 \leq m_3 \leq 4m_1^3 - 12m_1^2 + 9m_1. \tag{11}$$

Note that this is nonoverlapping with respect to the admissible m_1, m_3 values for the PP case. The plot of the constraint curves for m_3 versus m_1 in Fig. 3 indicates (and was confirmed analytically) that the range of possible m_3 yielding admissible solutions is maximized at $m_1 = 0.5$.

Then for $m_1 = 0.5$, as an example, the step angle solutions for θ_1 and θ_2 are as shown in Fig. 5 as m_3 varies. The solutions for θ_1 and θ_2 were also obtained at other allowable values of m_1 and m_3, but these are not shown here. Instead, we show the frequency-weighted THD, defined here as $\sqrt{\sum_{\text{odd}h=5}^{\infty}(V_h/h)^2}/\sqrt{V_1^2 + (V_3/3)^2}$, corresponding to these solutions (and to the solutions for the PP case) over a grid of m_1, m_3 values in Fig. 6. Note that the PN case requires the production of a three-level waveform and (at least) a one-cell converter. With a one-cell converter, the switches can be operated so that each turns on and off at twice the fundamental frequency. With a two-cell converter, it is possible to turn each switch on and off at the fundamental frequency to produce the desired waveform.

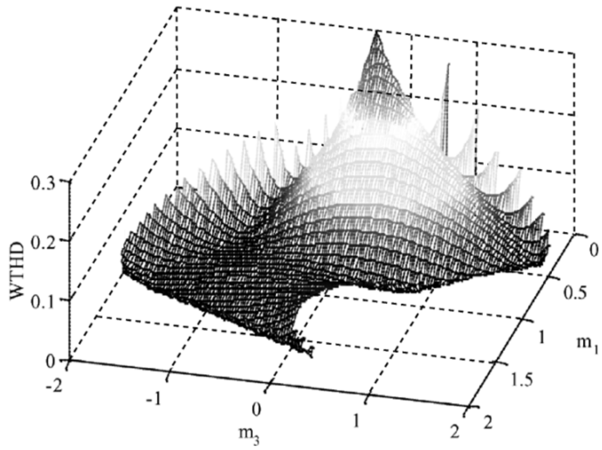

Fig. 6. Weighted THD plot for 2-step PP and PN cases combined.

B. Three-Step Waveform Problem

There are four, i.e., $1/2(2^3)$, possible combinations of three-step waveforms to consider, excluding those that are the negations of the following cases: PPP, PPN, PNP and PNN. The applicable equations are, from (5a), (5b) and (5c)

$$c_1 + k_2 c_2 + k_3 c_3 = m_1 \tag{12a}$$

$$\left(4c_1^3 - 3c_1\right) + k_2\left(4c_2^3 - 3c_2\right) + k_3\left(4c_3^3 - 3c_3\right) = 0 \tag{12b}$$

$$\left(16c_1^5 - 20c_1^3 + 5c_1\right) + k_2\left(16c_2^5 - 20c_2^3 + 5c_2\right) + k_3\left(16c_3^5 - 20c_3^3 + 5c_3\right) = m_5 \tag{12c}$$

where k_2, k_3 are either $+1$ or -1 for a positive or a negative step, respectively, and the objective is to produce desired levels of first and fifth harmonics with simultaneous elimination of the third. Substituting for c_3 from (12a) into (12b) and (12c) then yields two (multivariate) polynomial equations in terms of c_1 and c_2. The exact solution of such equations (as opposed to an iterative numerical search) is, in general, computationally intensive and increasingly difficult as the number of equations and variables increases [9], but it does yield *all* possible solutions. However, for two equations in two variables, the solution is relatively simple to obtain using any one of several alternative concepts such as the Gröbner basis [9] or the resultant polynomial [8], [9].

In each case, the region of m_1 and m_5 values yielding admissible solutions for c_1, c_2 and c_3 from (12) was first determined. Since the analytical determination of the constraint functions for such regions, as for the 2 step cases, becomes increasingly difficult as the number of step angles increases, a numerical method was used instead. Then with the admissible range of m_1 and m_5 known, the step-angles for various m_1 values were found by solving (12) iteratively for incrementally increasing values of m_5 that, again, allowed the frequency-weighted THD to be

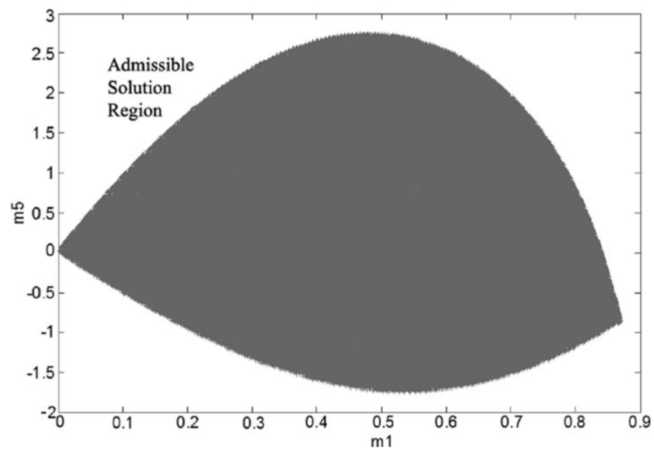

Fig. 7. Admissible region for m_5 versus m_1 (PNP case).

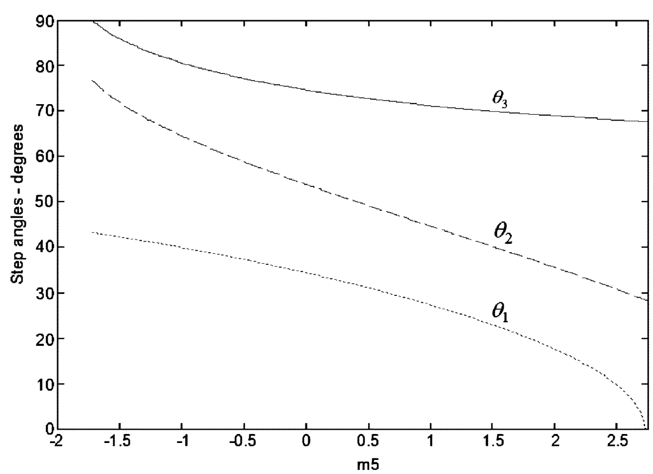

Fig. 8. Step angle solutions for $m_1 = 0.5$ (PNP case).

calculated (and plotted). Only the PNP case is briefly described here.

1) PNP Case: Solutions exist for the range of m_1 and m_5 indicated by the shaded region of Fig. 7. The value of m_1 yielding the maximum range of m_5 is about 0.5. The plot of the step-angle solutions at this value of m_1 is shown in Fig. 8. Note that this case requires the production of just a three-level waveform and (at least) a one-cell converter. But with a three-cell converter, it is possible to turn on and turn off each switch at the fundamental frequency to produce the desired waveform, which is impossible with a one- or two-cell converter.

C. Four-Step Waveform Problem

The above investigation was extended in a similar manner to the four-step/four-equation problem (corresponding exactly to (3) with $s = 4$) with desired levels of the first and third harmonics and simultaneous elimination of the fifth and seventh harmonics, and then to the problem of producing the first and fifth harmonics with simultaneous elimination of the third and seventh harmonics. Regarding the latter problem, Fig. 9 shows the admissible range of m_1 and m_5 for the four-step PNPP case.

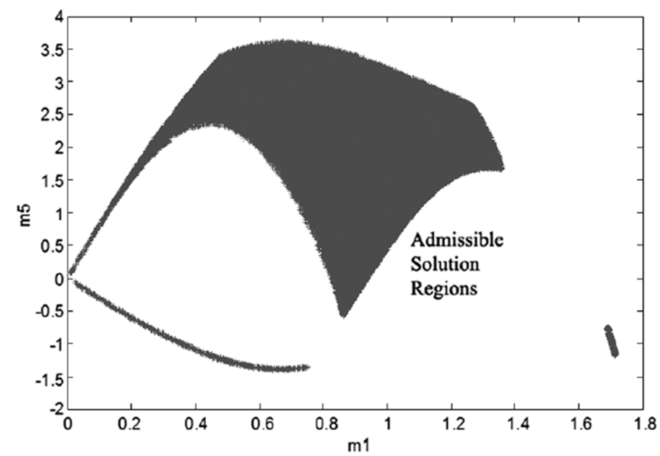

Fig. 9. Admissible region for m_5 versus m_1 (PNPP case).

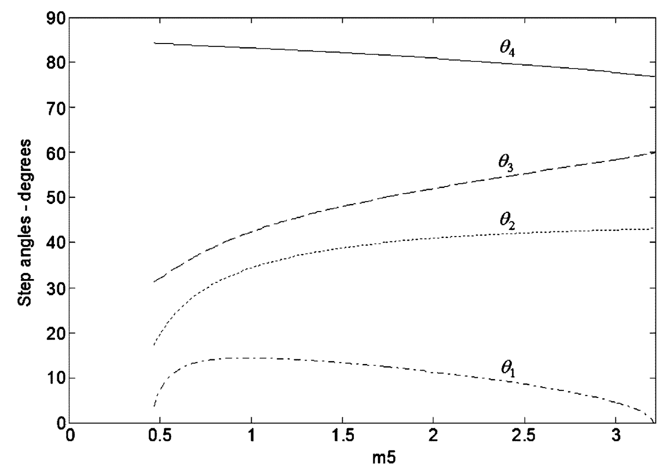

Fig. 10. Step angle solutions for $m_1 = 1$ (PNPP case).

The plot of the step-angle solutions for this case when $m_1 = 1$ is shown in Fig. 10.

III. Experimental Results

Laboratory measurements were obtained from a two-cell cascaded H-bridge inverter providing five levels of output, to demonstrate the PNPP case with the first and fifth harmonic voltages such that $V_1/V_5 = 5/3$ (so $m_1 = 1$, $m_5 = 3$) while eliminating the third and seventh harmonics. Note that the specific low and high frequency power levels applied in an induction heating application depend on several factors such as material and geometry but are typically on the order of 3:1. Fig. 11 shows the voltage and current waveforms for a fundamental frequency of 10 kHz. For this test, each dc voltage source was 125 V, the $(R - L)$ load average power was 513 W and the conversion efficiency was 91.3% (with each switch operating at 20 kHz). The step angles ($\theta_1 = 4.61°$, $\theta_2 = 42.89°$, $\theta_3 = 58.44°$, $\theta_4 = 77.73°$) were obtained from the data as plotted in Fig. 10. Table I indicates good agreement between the analytical and measured harmonic amplitudes. Note that in the current waveform, the higher harmonics are

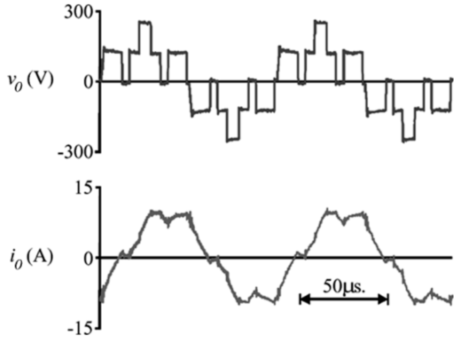

Fig. 11. Four-step, five-level inverter measurements.

TABLE I
FOUR-STEP, FIVE-LEVEL INVERTER VOLTAGE HARMONICS

	V_1	V_3	V_5	V_7	V_9	V_{11}
Analytical	159.1	0	95.5	0	3.2	7.5
Measured	156.8	2.7	98.1	2.2	3.0	10.1

mostly filtered out by the load inductance resulting mainly in the desired dual-frequency components.

IV. CONCLUSIONS

Fundamental results have been presented on the use of multilevel inverters for producing power at two frequencies simultaneously, as desirable for certain applications. Analysis has been performed for the two-step, three-step and four-step cases for equal dc sources. Furthermore, test results have been described for the four-step case that validates the proposed approach and corresponding analysis for dual-frequency voltage generation by multilevel inverters. Notable features of this approach include independent adjustability of the output voltage's first through seventh harmonics and reduced device switching frequency (when compared to the output's highest controlled frequency component), which are improvements over existing approaches. Work is presently underway to extend these results to the case of unequal dc sources.

REFERENCES

[1] K. Matsuse, K. Nomura, and S. Okudaira, "New quasiresonant inverter for induction heating," in *Proc. Power Conversion Conf.*, 1993, pp. 117–122.

[2] K. Matsuse and S. Okudaira, "Power control of an adjustable frequency quasiresonant inverter for dual frequency induction heating," in *Proc. PIEMC*, 2000, pp. 968–973.

[3] S. Okudaira and K. Matsuse, "Dual frequency output quasiresonant inverter for induction heating," *Trans. Inst. Elect. Eng. Jpn. D*, vol. 121, pp. 563–568, May 2001.

[4] K. Matsuse and S. Okudaira, "A new quasiresonant inverter with two-way short-circuit switch across a resonant capacitor," in *Proc. Power Conversion Conf.*, 2002, pp. 1496–1501.

[5] Simultaneous Dual Frequency Induction Heat Treating. [Online] Available: http://www.eldec.de/engl/download/SDF-method.pdf

[6] J. Rodriguez, J.-S. Lai, and F. Z. Peng, "Multilevel inverters: a survey of topologies, controls, and applications," *IEEE Trans. Ind. Electron.*, vol. 49, pp. 724–738, Aug 2002.

[7] J. I. Rodriguez and S. B. Leeb, "A multilevel inverter topology for inductively-coupled power transfer," in *Proc. IEEE/Conf. Applied Power Electronics*, 2003, pp. 1118–1126.

[8] J. Chiasson, L. Tolbert, K. McKenzie, and Z. Du, "Eliminating harmonics in a multilevel converter using resultant theory," in *Proc. IEEE Power Electronics Specialists Conf.*, 2002, pp. 503–508.

[9] D. Cox, J. Little, and D. O'Shea, *Using Algebraic Geometry*. New York: Springer-Verlag, 1998.